한국농림기상학회지, 제17권 제4호(2015) (pISSN 1229-5671, eISSN 2288-1859)
Korean Journal of Agricultural and Forest Meteorology, Vol. 17, No. 4, (2015), pp. 317~325
DOI: 10.5532/KJAFM.2015.17.4.317

A Feasibility Study of a Field-specific Weather Service for Small-scale Farms in a Topographically Complex Watershed

Jin I. Yun*
College of Life Science, Kyung Hee University, Yongin 17104, Korea
(Received October 16, 2015; Revised October 28, 2015; Accepted November 10, 2015)

지형이 복잡한 집수역의 소규모농장에 맞춘 기상서비스의 실현가능성

윤진일*
경희대학교 식물환경신소재공학과
(2015년 10월 16일 접수; 2015년 10월 28일 수정; 2015년 11월 10일 수락)

ABSTRACT

An adequate downscaling of synoptic forecasts is a prerequisite for improved agrometeorological service to rural areas in South Korea where complex terrains and small farms are common. In this study, geospatial schemes based on topoclimatology were used to scale down the Korea Meteorological Administration (KMA) temperature forecasts to the local scale (~30 m) across a rural catchment. Then, using these schemes, local temperatures were estimated at 14 validation sites at 0600 and 1500 LST in 2013/2014 and were compared with the observations. The estimation errors were substantially reduced for both 0600 and 1500 LST temperatures when compared against the uncorrected KMA products. The improvement was most notable at low lying locations for the 0600 temperature and at the locations on west- and south-facing slopes for the 1500 LST temperature. Using the downscaled real-time temperature data, a pilot service has started to provide the field-specific weather information tailored to meet the requirements of small-scale farms. For example, the service system makes a daily outlook on the phenology of crop species grown in a given field using the field-specific temperature data. When the temperature forecast is given for next morning, a frost risk index is calculated according to a known relationship of phenology and frost injury. If the calculated index is higher than a pre-defined threshold, a warning is issued and delivered to the grower's cellular phone with relevant countermeasures to help protect crops against frost damage.

***Key words*: Temperature downscale, Topoclimatology, Early warning system, Field-specific service, Climate extreme**

I. Introduction

Weather hazards affect production in uncontrollable ways, causing agriculture in particular to be vulnerable to climate extremes. Climate variability and the occurrence of extreme weather events caused by climate change are likely to increase, leading to a substantial increase in agricultural risk and destabilization of farm income (Gobin *et al*., 2013).

Risk management is a part of farmers' business strategies. Effective risk management involves the forecasting of possible weather hazards and the planning to

* Corresponding Author : Jin I. Yun
(jiyun@khu.ac.kr)

Fig. 1. Screen shots of typical farmland landscapes in the USA Midwest (left) and in South Korea (right) viewed from the same altitude (~1000 m).

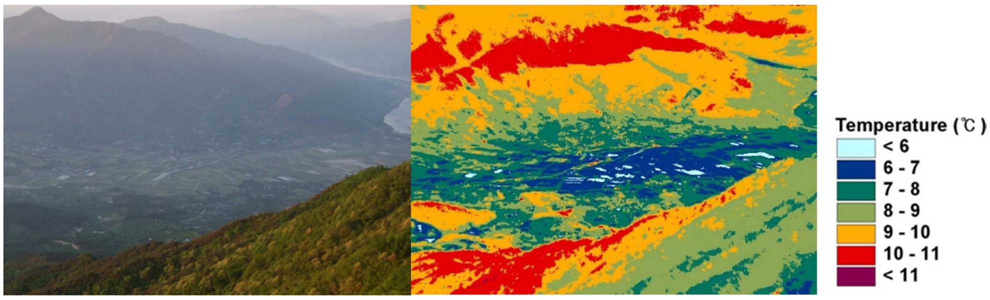

Fig. 2. A photograph of a typical watershed in South Korea (left), and a thermal image scanned across the valley at dawn on a spring day (right).

reduce the consequences. To facilitate farmers' risk management, national meteorological services in most countries operate a specific type of early warning system for the agricultural sectors. Despite various spatial scales of climate change and extreme weather events, their influences can only be detected on the local scale of farms and orchards. Therefore, national meteorological services have been increasing the spatial resolution of their weather products. Currently, regional models for operational use at weather services in developed nations provide their products at spatial resolutions down to 5-km over land and 10-km over oceans (Glahn and Ruth, 2003). Such levels of resolution might be sufficient for agricultural application in areas where large-scale farms lie over a nearly flat landscape (Fig. 1, left).

However, most of the rural communities in Korea are situated within small watersheds, and many small-scale farms lie over diverse locations within the watershed: lowlands near the outlet of the watershed, the side-slopes of the valley with contrasting aspects, and montane highlands (Fig. 1, right). The Korea Meteorological Administration (KMA) issues its digital forecast at the spatial resolution comparable to that of developed nations (~5 km). Considering the territory of South Korea (~99,000 km^2) and the number of watersheds including mountains and streams (~840), the average area per watershed is slightly more than 100 km^2. Hence, the average number of forecast grid cells falling within a watershed is approximately four. When a surface temperature map was produced across such a watershed using an infrared camera, we noticed substantial temperature variations which were not described by the pixels of the KMA digital forecast (Fig. 2).

Such a decoupling of near-surface microclimates from regional climates is well known over complex terrain because a small change in the surface energy budget can significantly alter the local environment (Barry 1992; Geiger *et al.,* 2003). Although the KMA digital forecast can capture the variation in regional-scale weather, its application to landscape-scale features (*i.e.*, agrometeorological forecasting for a farm or orchard) is limited. To assist small-scale farms located in a topographically complex watershed, topoclimatology - the study of how terrain influences local climate - should be revisited and used to complement existing synoptic products in South Korea.

The objectives of this study are: (1) to establish a topoclimatological method for near–real time downscaling of the KMA temperature products over complex terrain, (2) to test the performance of this method with respect to observed data at diverse locations in a topographically complex watershed, and (3) to show the feasibility of this method in near–real time temperature mapping over an extensive region at a resolution sufficient for field-specific agrometeorological forecasting.

II. Methods for Temperature Downscaling

2.1. Daily minimum temperature

The model selected for daily minimum temperature (T_n) estimation was based on the work of Chung *et al.* (2006), which added the correction terms for cold air drainage caused by nocturnal radiative cooling and the resultant thermal belt effect to a conventional lapse rate model (Thornton *et al*., 1997; Bolstad *et al*., 1998; Nalder and Wein, 1998). Chung *et al.* (2006) assumed cold-air flow to be the same as water flow, and the original model estimates the temperature decrease by considering cold-air accumulation at a given location as water-like free drainage.

The water-like free drainage assumption may not be valid for an enclosed catchment whose outlet is blocked by man-made obstacles such as banks and roads because cold air accumulates at the bottom. In order to describe the relative size of the temperature decrease for a range of catchment shapes, Kim and Yun (2011) modified the model by introducing a topographical variable (i.e., *shape factor*) which is the ratio of the cold air accumulation across the whole catchment area to the maximum capacity of the cold pool. In the modification, temperature decrease per unit volume varies among catchments depending on the topographic characteristics such as width, depth, slope, and shape.

In addition, Kim *et al*. (2012) found that daily minimum temperature in a cold pooling catchment does not decrease as predicted by this model when wind speed exceeds a certain threshold. They derived a linear regression equation to explain the warming effect of wind speed on daily minimum temperature based on the observations at a low lying location within an enclosed catchment.

In summary, the procedure for daily minimum temperature estimation in this study consists of the models by Chung *et al.* (2006), Kim and Yun (2011), and Kim *et al.* (2012).

2.2. Daily maximum temperature

Daily maximum temperature at a location differing in elevation from the nearest weather station (or a reference site) can be estimated using the lapse rate correction, and this method has been widely used by national meteorological services and private weather companies in order to improve their interpolated temperature products with respect to spatial representativeness over rugged terrain. However, assuming the same elevation with the reference, this site will have the same temperature regardless of its relative position on the slope, *i.e.*, this method produces the same results for southbound and northbound slopes.

As a method of estimating the daily maximum temperature for any sloping surface based on a nearby weather station, Regniere (1996) suggested a correction based on the solar irradiance deviation between the weather station and the sloping surface for the four hours between 1100 and 1500 LST. Chung *et al.* (2009) modified the correction according to the results from a field experiment conducted at a cone-shaped parasitic volcano in Jeju Island. Lately, Kim and Yun (2014) found that the temperature increase diminishes in an exponential way with the increase in wind speed and the solar radiation effect on the local temperature virtually disappears if the mean wind speed is greater than 3 m/s.

Hence, in this study, the method for estimating daily maximum temperature was based on the model of Regniere (1996), which was modified by Chung *et al.* (2009), with addition of the advection function by Kim and Yun (2014).

III. Validation of the Downscaled Temperatures

3.1. Study area and data acquisition

The Akyang watershed, located in the south of the

Jiri Mountain National Park and one of the 840 standard watersheds in South Korea, was selected as the study area for model validation. Though it has a rather small catchment area of 54 km^2, its topography is complex with an elevation range of 5 to 1120 m above mean sea level and diverse sloping aspects. Because the minimum temperature estimation model uses the flow accumulation function available in most geographical information system (GIS) software, a watershed with natural hydraulic divides is appropriate for model application.

The weather data were collected from the automated weather stations (STA Corporation, Anyang, Korea) installed at 14 sites with an elevation range of 10 to 1100 m above sea level from 5 July 2013 to 31 December 2014. At each site, the air temperature and relative humidity, wind speed and direction, rainfall, and solar radiation were measured at 1-minute intervals and transmitted to a remote laboratory every 10 minutes.

The 14 observation sites were distributed on the western and eastern slopes divided by a stream that flows from north to south. Sites 5 and 7 were at the same altitude of 280 m, but site 5 was located on the west-facing slope and site 7 on the east-facing slope. The altitude of site 4 on the west-facing slope was 326 m, similar to that of site 14 on the east-facing slope. Site 2 on the west-facing slope (92 m above sea level) and site 9 on the east-facing slope (105 m above sea level) had a relatively gentle slope compared with those at higher altitudes. Site 6 had an easy south-facing slope located near the valley bottom. Sites 1 and 10 had a southeast-facing slope with an altitude of 40 m. The altitude of site 11 was 10 m above sea level making the lowest in the study area and site 13 was located on the mountain peak (1100 m above sea level) just outside the study area (Fig. 3).

During the same period, the solar radiation, sunshine duration, and cloud data were collected from the near-

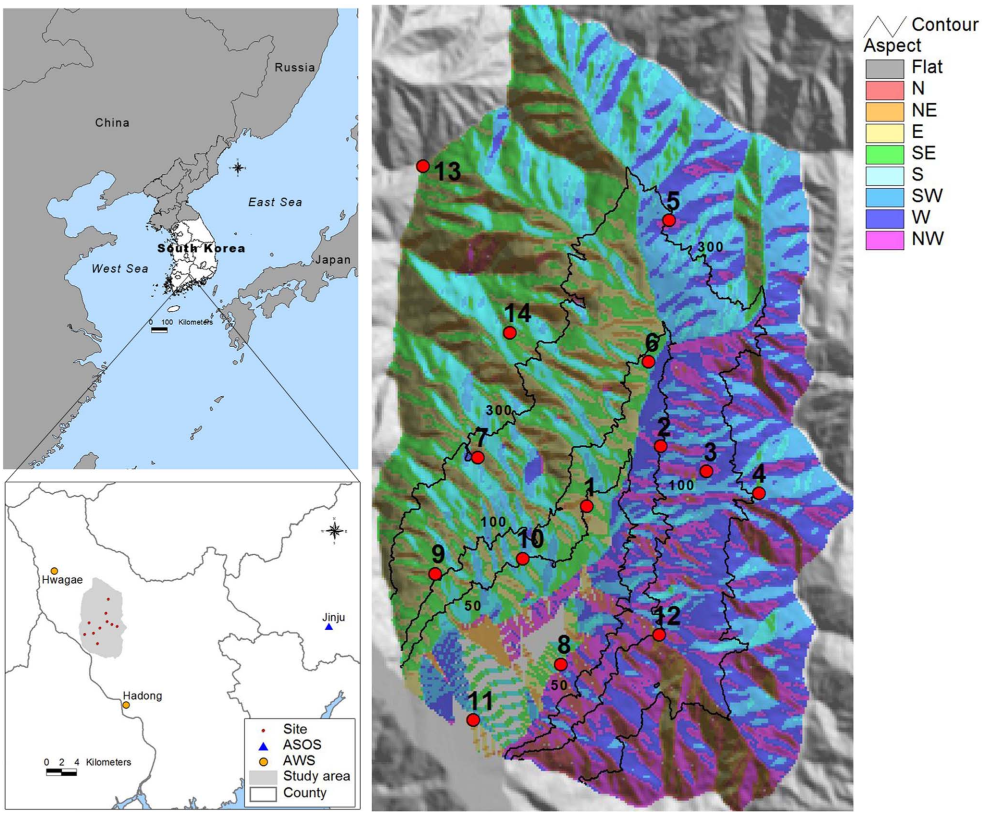

Fig. 3. The slope aspect of the study area based on a 30 m × 30 m digital elevation model (right). The red circles represent the locations of the validation sites (Site), and the black lines are elevation contours in meters. The locations of the two nearest automated weather stations (AWS) and one synoptic station (ASOS) of the Korea Meteorological Administration are depicted in the left panel.

est synoptic KMA weather station (Jinju), which was 30 km from the study area. Those data were considered to represent the atmospheric conditions over the study area. Days with an average cloud amount less than 1 and more than 9 on a 0 (clear) to 10 (overcast) scale were selected by calculating the average values of four daily observations (1200, 1300, 1400, and 1500 LST) in order to classify clear and cloudy days.

3.2. Validation of temperature estimates

We calculated daily minimum temperatures at the 14 validation sites from 5 July 2013 to 31 December 2014, following Chung *et al.* (2006), Kim and Yun (2011), and Kim *et al.* (2012). The results were compared with the observations. Details on the calculation procedures are as follows.

Background temperature estimates were calculated daily by averaging the two KMA AWS observations (Hwagae and Hadong in Fig. 3) at 0600 LST. Portions of the 30-m DEM of South Korea (http://www.egis.go.kr) corresponding to the study area were clipped and regarded as the actual terrain. Elevation differences at the 14 DEM grid cells for validation were obtained as the difference between the actual terrain and the elevation surface of the virtual terrain prepared by an IDW interpolation of the elevations of the two KMA AWS's. Flow accumulation at each site was calculated from the 30-m DEM using the coordinate data and flow direction grid. The cold air accumulation across the whole catchment area and the maximum capacity of the cold pool were calculated from the 30-m DEM using the cut and fill function of ArcGIS (Release 9.3, ESRI, Redlands, California, USA).

A dry adiabatic lapse rate (-0.0098°C/m) was applied to the elevation difference. Daily temperature range was assumed to be the mean difference between the maximum temperature of the previous day and the minimum temperature of the present day as observed at the two KMA AWS's. The wind speed term was substituted with the hourly mean of site observations at 0600 LST. The background temperature estimates were corrected for cold air drainage and cold pool effects, resulting in daily site-specific temperature estimates at 0600 LST.

The method based on Chung *et al.* (2009) modified by Kim and Yun (2014) was used to obtain the 1500 LST temperature estimation at the 14 sites from 5 July 2013 to 31 December 2014. The results were compared with the observations. First, the mean of the 1500 LST temperatures observed at two automated KMA weather stations (Hwagae and Hadong in Fig. 3) was set as the background temperature of the study area. The 1500 LST temperature deviation between the mean altitude of the two automated weather stations and the altitude of the 14 sites presented by the 30-m DEM was corrected using a dry adiabatic lapse rate, as with daily minimum temperature. Additional details on the calculation procedures are as follows.

The hourly solar irradiance at each site (including the reference) was calculated using the method of Kondratyev and Federova (1977) and accumulated from 1100 to 1500 LST. In this process, the topography of the study area was represented by the 30-m DEM, but areas smoothed to a radius of 750 m (*i.e.*, 25 DEM cells) were used for the slope and aspect calculation following the suggestion of Kim and Yun (2013). Extraterrestrial daily radiation was estimated for the center of the study area (35° 10' 00"N and 127° 43' 00"E) from January 1 to December 31 using the method of Allen *et al*. (1998), and the same value was used regardless of the site location. Observed wind speed at the 14 sites for 1100-1500 LST was used to calculate the wind speed correction factor, which was then applied to the solar radiation effect.

We compared the maximum and minimum temperatures predicted by our method with those measured at each site and calculated the bias (mean error, ME) and root mean square error (RMSE).

IV. Application to a Field-specific Service

The National Center for Agro-Meteorology (NCAM), a joint initiative of the Rural Development Administration, Korea Forest Service, Seoul National University, and KMA, designed a risk management solution for small-scale farms threatened by climate change and variability (Yun *et al*., 2013). The core of the solution is an innovative service that provides agrometeorological information tailored to a farmer's need with respect to crop species and phenology on an individual farm basis. If the risk is high enough to cause any damage to the crops, a warning or watch shall be delivered to the farmer's cell phone with a short message describing relevant countermeasures to help protect the crops against the potential damage. A prerequisite to this service is, of course, site-specific weather forecasts and analysis at a high spatial resolution, which is unobtainable in the existing products from either the KMA or private companies. We decided to apply our temperature downscaling methods to KMA digital products to demonstrate the feasibility of producing fine-grain temperature surfaces over a large area (> 300km^2) at a near–real time basis (< daily).

Our selected service region was the Lower Seomjin River Basin (LSRB) consisting of three watersheds (~350 km^2 area). It is a mixed farmland and forest region with a complex terrain. Temperate fruits such as pears, persimmons, apricots, and chestnuts as well as subtropical crops like tea and malting barley are some of the major products from this region. Due to the topographical complexity, this region shows a diversity of local climates and more frequent weather extremes than comparable plains in the vicinity. For example, nocturnal cold-air pools frequently form in this region under anticyclonic systems and are a hazard to the flowering buds of temperate fruit trees as well as to the winter survival of subtropical species. Most deciduous fruit tree species require a minimum accumulation of winter chilling temperature units to break dormancy, which can be estimated by daily maximum and minimum temperatures (Chung *et al*., 2006). Therefore, a frost warning system could be operated within the NCAM service in this region if site-specific temperature forecasts were available on a near–real time basis.

The spatial distribution of daily maximum and minimum temperatures at a 30 m × 30 m resolution was produced for the LSRB based on the KMA digital forecasts (up to a 10-days lead time), *i.e*., the background temperature for initialization was replaced with the 5-km resolution KMA products. In addition, the 5-km KMA wind field was downscaled to 270 m resolution using the MUKLIMO micro-scale urban climate model (Sievers and Zdunkowski, 1986) to provide the wind

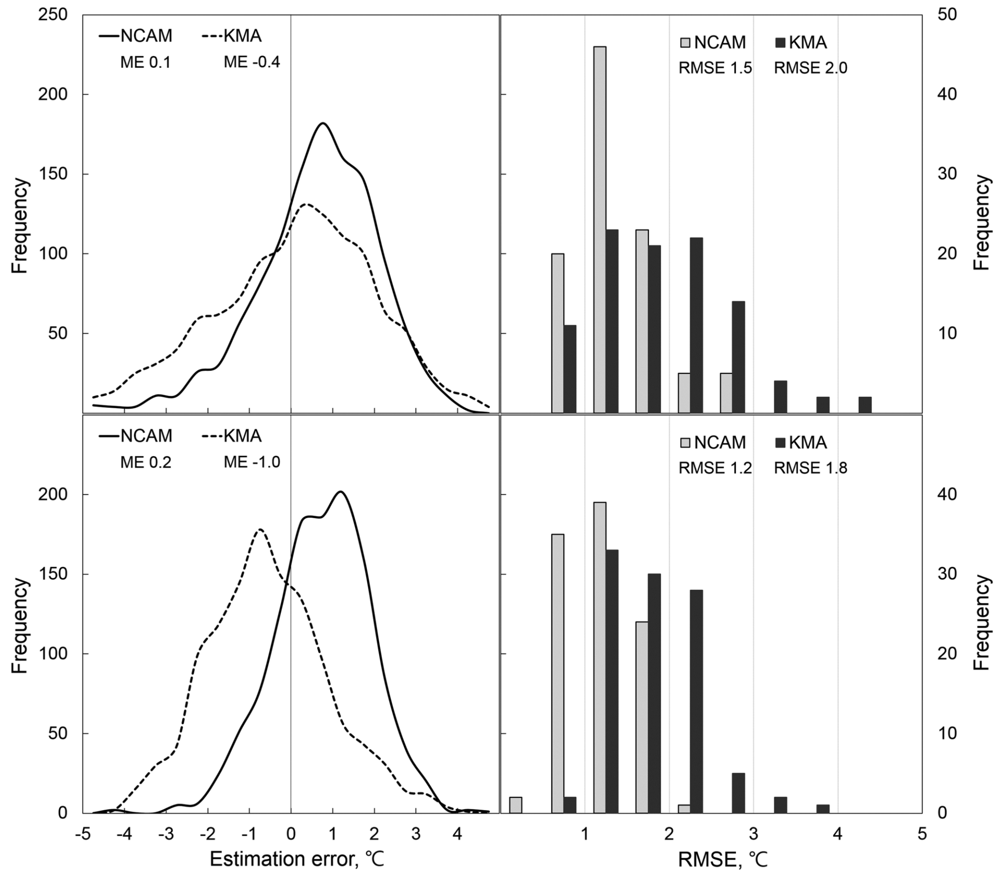

Fig. 4. Frequency distributions of the estimated minus observed temperature differences at 14 validation sites on 101 cloudless days (left) and histograms of the root mean square errors across the14 sites in 0.5°C intervals (right). Upper and lower panels represent daily minimum (0600 LST) and maximum (1500 LST) temperatures, respectively.

data necessary to correct for both the cold pool effect on daily minimum temperatures and the solar radiation effect on daily maximum temperatures. Also, the reference solar radiation for calculating the irradiance on sloping surfaces was replaced by hourly observations at the nearest synoptic station (Jinju), which sits 30-km east of the service region. All the geospatial data preparation and temperature calculation procedures were written in C++ and embedded in the NCAM service system. The system was run twice a day with the

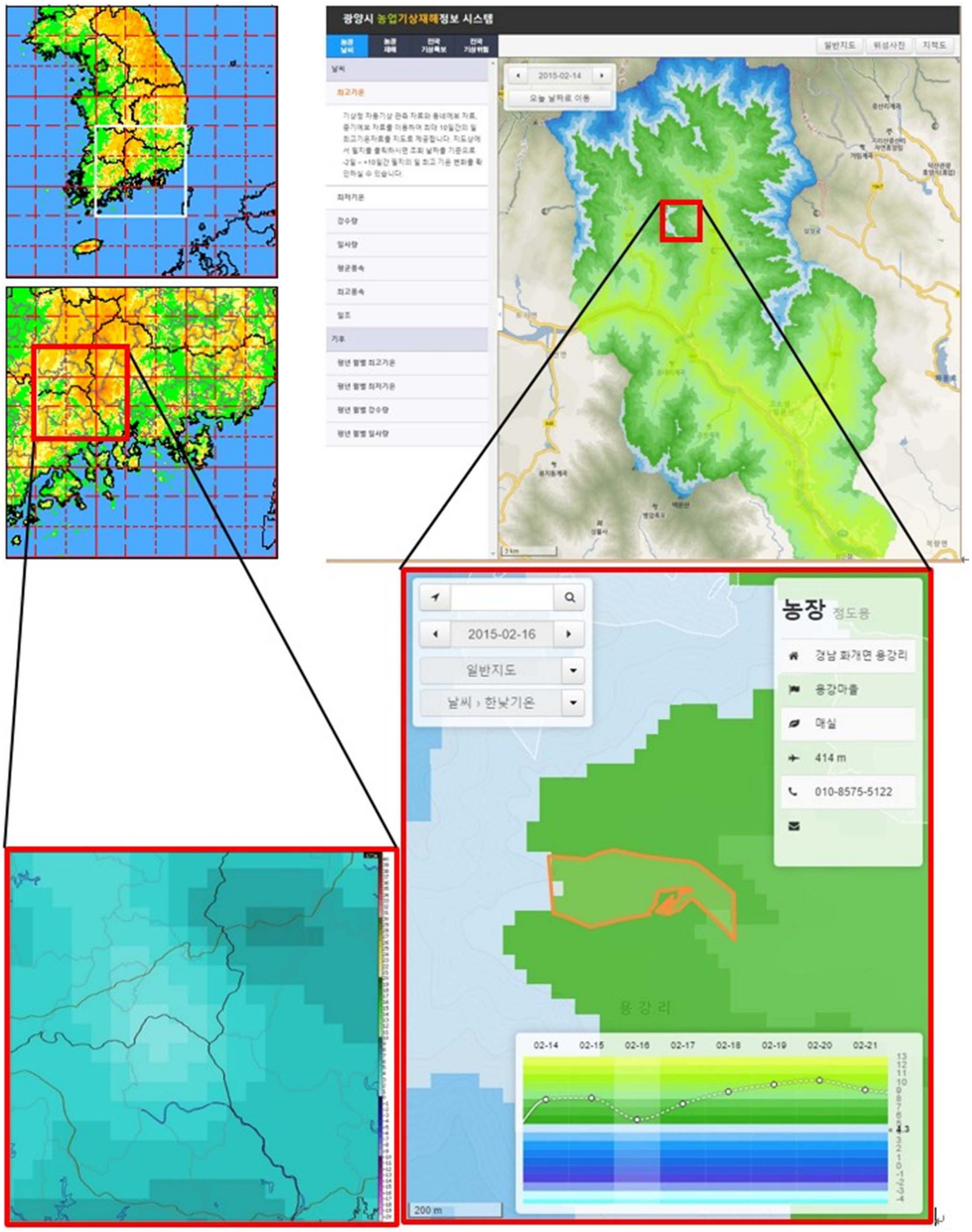

Fig. 5. Near–real time temperature maps for the study area provided by the Korea Meteorological Administration (KMA, left panel) and the National Center for Agro-Meteorology (NCAM, right panel), respectively. An individual farm (orange) can be identified on the NCAM map at the 30-m resolution (bottom right), whereas few landscape-scale features can be detected on the KMA map even at its maximum resolution of 5-km (bottom-left).

updated KMA digital products, delivering text-based field-specific information to the relevant farmers and providing web-based graphic information to the public.

V. Results and Discussion

5.1. Performance of temperature models

On the 77 overcast days during the study period (5 July 2013-31 December 2014), the KMA products showed a good agreement with the observations both in 0600 and 1500 LST temperatures. The RMSE was 1.0°C for the 0600 LST and 1.1°C for the 1500 LST temperatures, whereas our method using the topoclimatic correction showed little improvement over these values. On the 101 cloudless days, however, the RMSE of KMA products increased to 2.0°C for the 0600 LST and 1.7°C for the 1500 LST temperatures, respectively. Moreover, significant biases with the ME of -0.4°C for 0600 LST and -1.0°C for 1500 LST temperatures were noted under this condition (Fig. 4).

Uncorrected KMA minimum temperatures showed overestimation at the sites on the valley bottom where cold-air pooling was frequent and underestimation at the side slopes with a 250 to 300 m elevation range (thermal belt), setting off the ME value. With our method, we estimated site-specific minimum temperatures at the 14 sites with an RMSE of 1.3°C regardless of sky condition during the study period. This level of estimation error seems similar to that for the KMA products (1.5°C), but the cloudless-day-only data showed a remarkable difference between the two. The RMSE for the 0600 LST temperature was 1.5°C with our method applied to the 101 cloudless days, whereas that of the KMA products increased to 2.0°C.

The bias of the uncorrected KMA maximum temperatures represents a substantial underestimation (lower left panel, Fig. 4), and this tendency was most remarkable at the sites on west- and south-facing slopes. A farmer with a farm on the west- or south-facing slopes who uses the KMA maximum daily temperature data to manage the heat stress on his crops or animals will be exposed to higher risk of failure than nearby farmers working on the farms with different sloping aspects. On the other hand, our method showed a ME of 0.2°C, eliminating virtually all the negative bias caused by the KMA method. The RMSE for the 1500 temperature was 1.2°C, showing a consistent performance regardless of sky condition.

5.2. Field-specific services

Our models were implemented within the NCAM system serving more than 400 volunteer farmers in a 350-km^2 rural area with diverse agricultural activities (http://www.agmet.kr). The farmers are alerted by cellular phone messages with field-specific weather information and assisted with countermeasures tailored to their crops. They also feed their evaluations back to NCAM for further improvement. In addition, the public can access the near–real time temperature maps for the study area and identify individual farms (Fig. 5). This feature is most remarkable when compared with the KMA digital products, in which few landscape-scale features can be detected even at its maximum resolution of 5-km.

Currently, several temperature-driven products are in service, such as forecasting of phenology (*e.g.*, date for dormancy break, budburst, and flowering). In conjunction with other meteorological variables, fine-grain temperature data are expected to produce a diversity of field-specific agrometeorological information ranging from drought monitoring to plant disease and pest forecasting. The experience obtained through this study will be useful in planning and developing a nationwide early warning service for the agricultural sector, exposed as it is to increasing hazards from climate and weather extremes.

적 요

우리나라 농촌은 지형이 복잡하고 소규모 농장이 많아 농업기상서비스 개선을 위해서는 먼저 기상청 종관예보의 규모축소가 필요하다. 지형기후학에 근거한 공간정보기술을 이용하여 기상청의 기온예보자료 가운데 0600과 1500 LST자료를 선정된 집수역에 대해 30 m급의 국지규모로 상세화하고, 14개 관측소의 실측기온자료를 2013년부터 2014년까지 수집하여 비교하였다. 그 결과 0600 LST기온의 경우 집수역 가운데 고도가 낮은 곳에서, 1500 LST 기온의 경우 계곡의 서향 및 남향 사면에서 정확도가 크게 개선되는 것을 확인하였다. 상세화 한 기온실황자료를 이용하여 지역 내 소규모 농장을 대상으로 하는 시범서비스를 시작하였으며 농장 맞춤 기상정보를 제공하고 있다. 예컨대 이 서비스시스템은 기온자료를 토대로 작물의 발육단계를 추정하고, 발육단계별 최저기온에 따른 서리해 발생 관계식에 의해 내일 아침 예보기온의 서리위험 여부를 판정한다. 만약 서리위험도가 미리 설정된 기준을 넘으면 농장주의 휴대폰으로 대응지침과 함께 서리해 경보를

발송하여 피해를 예방할 수 있도록 도와준다.

Acknowledgements

This work was carried out with the support from the "Cooperative Research Program for Agricultural Science & Technology Development (Project No. PJ010007)" of Rural Development Administration, Republic of Korea.

REFERENCES

Allen, R. G., L. S. Pereira, D. Raes, and M. Smith, 1998: *Crop Evapotranspiration: Guidelines for Computing Crop Water Requirements.* FAO irrigation and drainage paper 56. UN-FAO, Rome, Italy, 333 pp.

Barry, R. G., 1992: *Mountain Weather and Climate*. 2nd ed. Routledge, 402 pp.

Bolstad, P.V., L. Swift, F. Collins, and J. Regniere, 1998: Measured and predicted air temperatures at basin to regional scales in the southern Appalachian Mountains. *Agricultural and Forest Meteorology* **91**, 161-176.

Chung, U., H. H. Seo, K. H. Hwang, B. S. Hwang, J. Choi, J. T. Lee, and J. I. Yun, 2006: Minimum temperature mapping over complex terrain by estimating cold air accumulation potential. *Agricultural and Forest Meteorology* **137**, 15-24.

Chung, U, H.-C. Seo, J. I. Yun, S.-J. Jeon, K. H. Moon, H.-H. Seo, and Y. S. Kwon, 2009: Extrapolation of daily maximum temperature in a mountainous terrain. *Asia-Pacific Journal of Atmospheric Sciences* **45**, 473-482.

Fridley, J. D., 2009: Downscaling climate over complex terrain: High finescale (<1000 m) spatial variation of near-ground temperatures in a montane forested landscape (Great Smoky Mountains). *Journal of Applied Meteorology and Climatology* **48**, 1033-1049.

Geiger, R., R. H. Aron, and P. Todhunter, 2003: *The Climate near the Ground*. 6th ed. Rowman and Littlefield, 584 pp.

Glahn, H. R., and D. P. Ruth, 2003: The new digital forecast database of the National Weather Service. *Bulletin of American Meteorological Society* **84**, 195-201.

Gobin, A., A. M. Tarquis, and N. R. Dalezios, 2013: Weather-related hazards and risks in agriculture. *Natural Hazards and Earth System Science* **13**, 2599-2603.

Jarvis, C. H., and N. Stuart, 2001: A comparison among strategies for interpolating maximum and minimum daily air temperatures. Part I: The selection of "Guiding" topographic and land cover variables. *Journal Applied Meteorology* **40**, 1060-1074.

Kim, S. O., J. H. Kim, D. J. Kim, and J. I. Yun, 2012: Wind effect on the distribution of daily minimum temperature across a cold pooling catchment. *Korean Journal of Agricultural and Forest Meteorology* **14**, 277-282. (in Korean with English abstract), DOI: 10.5532/KJAFM.2012.14.4.277.

Kim, S. O., and J. I. Yun, 2011: A quantification method for the cold pool effect on nocturnal temperature in a closed catchment. *Korean Journal of Agricultural and Forest Meteorology* **13**(4), 176-184. (in Korean with English abstract), DOI: 10.5532/KJAFM.2011.13.4.176.

Kim, S. O., and J. I. Yun, 2013: Relationship between midday air temperature and solar irradiance over sloping surfaces under cloudless conditions. *Korean Journal of Agricultural and Forest Meteorology* **15**, 291-297. (In Korean with English abstract), DOI: 10.5532/KJAFM.2013.15.4.291.

Kim, S. O., and J. I. Yun, 2014: Improving usage of the Korea Meteorological Administration's digital forecasts in agriculture: III. Correction for advection effect on determination of daily maximum temperature over sloped surfaces. *Korean Journal of Agricultural and Forest Meteorology* **16**(4), 297-303.

Kondratyev, K. Y., and M. P. Federova, 1977: *Radiation Regime of Inclined slopes.* WMO Technical Note No. 152.

Nalder, I. A., and R.W. Wein, 1998: Spatial interpolation of climatic normals: test of a new method in the Canadian boreal forest. *Agricultural and Forest Meteorology* **92**, 211-225

Regniere, J., 1996: A generalized approach to landscape-wide seasonal forecasting with temperature-driven simulation models. *Environmental Entomology* **25**, 869-881.

Sievers, U., and W. G. Zdunkowski, 1986: A micro-scale urban climate model. *Beiträge zur Physik der Atmosphäre* **69**(1), 13-40.

Thornton, P. E., S. W. Running, and M. A. White, 1997: Generating surfaces of daily meteorological variables over large regions of complex terrain. *Journal of Hydrology* **190**, 214-251.

Yun, J. I., S. -O. Kim, J.-H. Kim, and D.-J. Kim, 2013: User-specific agrometeorological service to local farming community: a case study. *Korean Journal of Agricultural and Forest Meteorology* **15**, 320-331. (In Korean with English abstract), DOI: 10.5532/KJAFM.2013.15.4.320.